Abdominal Radiology (2019) 44:3858–3873
https://doi.org/10.1007/s00261-019-02148-3

SPECIAL SECTION: UROTHELIAL DISEASE

Advanced urothelial cancer: a radiology update

Francesco Alessandrino[1,2] · Ola Ghaith[1,2] · Kristin Williams[1,2] · Guru P. Sonpavde[3] · Stuart G. Silverman[2] · Atul B. Shinagare[1,2]

Published online: 30 July 2019

Abstract
The recent genomic characterization of urothelial carcinoma by the Cancer Genome Atlas Project, made possible by the introduction of high throughput, reduced cost, and sequence analysis, has shed new insights on the biology of advanced disease. In addition, studies on imaging of advanced urothelial carcinoma have widened the knowledge on disease presentation and on pattern of metastatic spread and their correlation with the underlying biology of urothelial carcinoma. The wide range of treatments for advanced urothelial cancer, including combined chemotherapy regimens and immune checkpoint inhibitors, each result in treatment class-specific patterns of response and adverse events. Results of studies point to the need for a reliable biomarker, perhaps with imaging, that predicts prognosis and treatment response to systemic treatment, and can be used to select the most effective treatment while minimizing toxicity. This review of advanced urothelial cancer introduces the latest advances in genetic profiling, the current role of imaging, the radiographic appearance of treatment response and their toxicities, and details potential future areas of imaging research.

Keywords Urothelial carcinoma · Transitional cell · Urinary bladder neoplasms · Computed tomography · X-ray · Programmed cell death-1 receptor · Neoplasm · Metastasis

Introduction

Urothelial carcinoma (UCa) can be divided into bladder cancer, consisting of 90–95% of UCa, and upper tract urothelial carcinoma (UTUCa), which comprise the remaining 5–10% [1, 2]. UCa is considered 'advanced' when it has spread to lymph nodes or to distant organs, such as the lungs, bones or liver. The American Cancer Society estimates that in 2019, there will be 17,670 deaths from 80,470 new cases of UCa, making this cancer the sixth most common cause of cancer deaths [3]. Although advanced UCa is a fatal disease, recent genomic characterization by The Cancer Genome Atlas (TCGA) Project has shed new light on the tumor biology of advanced UCa, with new mutations and new targetable cell survival pathways identified [4, 5]. Recent studies on imaging presentation of disease and on pattern of metastatic spread have elucidated the correlation with the underlying biology of UCa [6]. Therapeutic options have evolved from a better understanding of the genetics of UC. Although conventional chemotherapeutic agents are still commonly used as initial treatment of UCa, five immune checkpoint inhibitors have been approved by the Food and Drug Administration (FDA) for treatment of unresectable locally advanced or metastatic disease in the past 2 years [7].

The role of imaging has also evolved from staging and detection of advanced disease to treatment response assessment as well as the identification of adverse events due to the treatment [8]. Thus, knowing the available specific treatment options, how to use imaging to assess response and recognizing drug-associated adverse events is crucial to the radiologist and other physicians who care for patients with UCa. This review of advanced UCa after introducing the latest developments in genetic profiling, will focus on the current role of imaging, the radiographic appearance of treatment

✉ Francesco Alessandrino
falessandrino@bwh.harvard.edu

[1] Department of Imaging, Dana Farber Cancer Institute, Harvard Medical School, 450 Brookline Avenue, Boston, MA 02215, USA

[2] Department of Radiology, Brigham and Women's Hospital, Harvard Medical School, 75 Francis Street, Boston, MA 02115, USA

[3] Lank Center for Genitourinary Oncology, Dana Farber Cancer Institute, Harvard Medical School, 450 Brookline Avenue, Boston, MA 02215, USA

response and their toxicities, and will detail potential future areas of imaging research.

Genetic profile of urothelial cancer

Bladder cancer and UTUCa each have different genomic expressions [9, 10]. Bladder cancer develops via two distinct cancer cell growth pathways, giving rise to papillary non-muscle-invasive tumors (NMIBC) and non-papillary muscle-invasive tumors (MIBC), each characterized by different pathophysiology and different underlying genomic alterations (Fig. 1) [5, 11, 12].

NMIBC tumors arise from hyperplastic or minimally dysplastic urothelium, are characterized by loss of heterozygosity at chromosome 9, by activating mutations of FGFR3, TERT, PI3KCA and by inactivating mutation in STAG2, all of which promote cell proliferation, division and growth. MIBC arise from severe dysplastic urothelium or from carcinoma in situ. Unlike NMIBC, these tumors show TP53 mutations, and fewer FGFR3 mutations. NMIBCs might progress to MIBC, due to loss of the tumor suppressor CDKN2A [11].

Most advanced UCa arises from MIBC now thought to be one of the cancers with highest mutation frequency [5, 11, 13]. Mutational load, defined the amount of mutations present in a cancer, is often related to mutations in genes coding for the apolipoprotein B mRNA editing catalytic polypeptide-like (APOBEC) family of enzymes in bladder cancer: in the TCGA study, MIBC with APOBEC-related high mutational load was associated with increased overall survival and were correlated with immunogenic response of the tumor, suggesting the role of mutational load as a potential biomarker of response to immune checkpoint inhibitors [5, 12, 14, 15].

Per TCGA, five subtypes of MIBC have been identified based on RNA expression, which correlate with outcomes and might guide treatment: basal-squamous, luminal-infiltrated, luminal and luminal-papillary and neuronal, with different genetic make-up with potential implications for treatment selection (Table 1) [5, 16–18].

Basal-squamous subtype shows frequent mutations in TP53, high immune infiltrations, elevated Programmed Death Ligand-1 (PD-L1), as well as high epithelial growth factor receptor (EGFR) expression [5, 16, 19]. The basal subtype may be particularly sensitive to cisplatin-based chemotherapy as well as PD1/PD-L1 inhibitors [5, 20]. The luminal-infiltrated subtype is enriched in FGFR3 activating mutation as well as PTEN, RB1, and TP53 mutations [12, 16]. This subtype shows high lymphocytic infiltration and good response to PD-1/PD-L1 inhibitors [5, 16, 21, 22]. Luminal-papillary subtype shows overexpression of FGFR3, making this subtype a target for anti-FGFR3 tyrosine kinase inhibitors [12, 23]. The luminal subtype shows high expression of uroplakins (UPK1A, UPK2) and Human Epidermal Growth Factor Receptor 2 (HER-2) alterations, with possible role of HER-2-targeting drugs and good response to neoadjuvant chemotherapy in MIBC [24, 25]. Neuronal subtype,

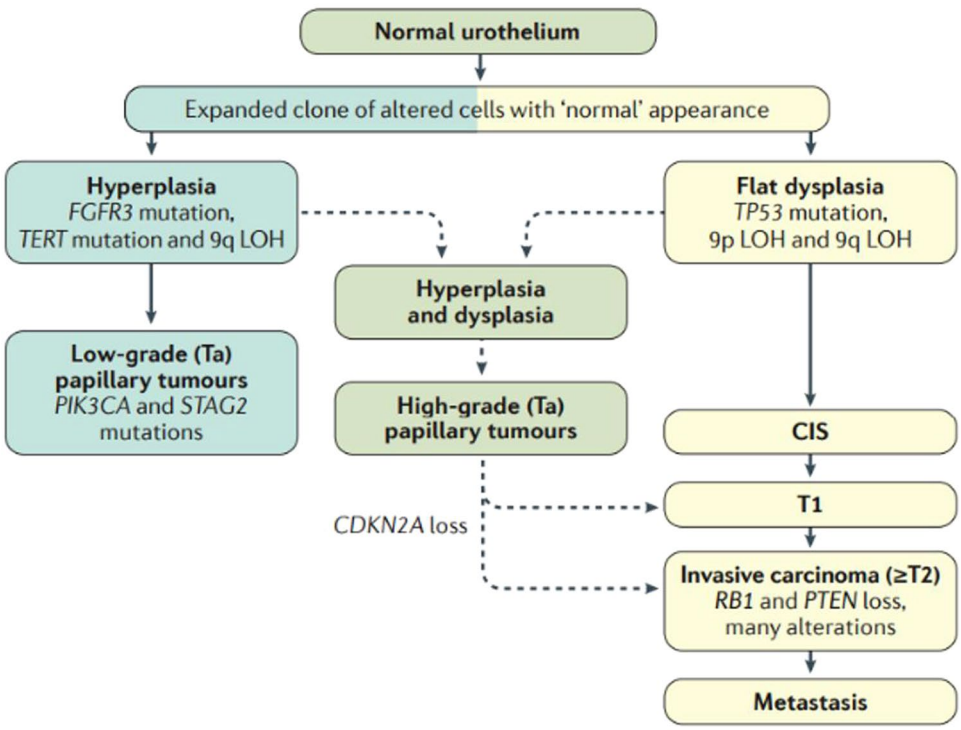

Fig. 1 Urothelial cancer pathogenesis pathways. Non-muscular invasive bladder cancer (NMIBC) pathway is shown in turquoise, muscular invasive bladder cancer (MIBC) pathway is shown in yellow. Solid arrows indicate pathways with histopathological or molecular evidence; dashed arrows indicate uncertainty. *LOH* loss of heterozygosity, *CIS* carcinoma in situ. (Reproduced with permission from Sanli O. et al., Nat Rev Dis Primers 2017; Springer nature)

Table 1 Molecular subtypes of bladder cancer according to The Cancer Genome Atlas, associated genetic characteristics, actionable targets, and clinical features [TCGA]

Subtype	Genetic characteristics	Actionable targets	Clinical features	Frequency (%)
Basal-squamous	Frequent P53 mutations	EGFR PD-L1 and CTLA-4	More common in women Good response to PD-1/PD-L1 and EGFR inhibitors	35
Neuronal	Loss of TP53 and RB1	WNT/b-catenin	Similarities with neuroendocrine tumors Poor survival	5
Luminal-infiltrated	High EMT expression	PD-L1 and CTLA-4	Good response to PD-1/PD-L1 inhibitors	19
Luminal	High UPK1A, UPK2 expression	HER-2	Good response to neoadjuvant chemotherapy	6
Luminal-papillary	High FGFR3 expression	FGFR3	Tumors enriched in papillary features	35

EGFR epithelial growth factor receptors, *EMT* epithelial-to-mesenchymal transition, *FGFR3* fibroblast growth factor receptor 3, *PD-1/PD-L1* programmed death/programmed death ligand-1, *HER-2* human epidermal growth factor receptor 2, *CTLA-4* cytotoxic T-lymphocyte-associated protein 4

the least common, shows features similar to neuroendocrine tumors and mutations in WNT/b-catenin signaling pathway, and recent data indicate exquisite sensitivity to PD1/PD-L1 inhibitors in this rarer subset [5, 26, 27]. Gene expression signatures consistent with epithelial-mesenchymal transition (EMT) and transforming growth factor β (TGFβ) signaling also appear to be associated with poor response to PD1/PD-L1 inhibitors [28, 29].

Advanced UTUCa have a distinct mutation profile and are characterized by frequent mutations in FGFR3, KMT2D, PIK3CA, and TP53 [30].

Role of imaging

Imaging is crucial for the management of patients with UCa [31]. The goals of staging are to determine the clinical TNM stage—for bladder cancer, detail the extent of involvement of the bladder, for UTUCa, detail the involvement of the renal pelvis, ureter, and the extension peripelvic fat or renal parenchyma and to assess for both the regional adenopathy and metastatic disease. Staging typically includes CT of the chest, and CT or MRI of the abdomen and pelvis. Protocols that results in CT urography (CTU) or MR urography (MRU) help identify synchronous tumors of the upper tract, which occurs in up to 4% patients with bladder cancer and 30% of patients with UTUCa [31, 32]. With respect to bladder wall involvement, MRI is preferred as it can be used to image muscle wall layers, whereas for ureter or intrarenal collecting system involvement, CTU is preferred; MRU can be used if CTU is contra-indicated (Fig. 2) [32–34].

In patients with advanced UCa undergoing systemic therapy, CT of the chest and CT or MRI of the abdomen and pelvis (preferably with CTU or MRU) are typically obtained at 3- to 6-month intervals for 2 years, and annually for the subsequent 5 years to both assess treatment response and identify metachronous tumors [31, 35]. Bone scintigraphy may be helpful in patients with bone pain, elevated alkaline phosphatase, or new fractures [31]. MRI of the brain can be performed for neurologic symptoms [31, 36, 37]. Although CT and MRI are the preferred staging modalities, 18-FDG PET/CT may be useful also [31, 37]. In addition, 18-FDG PET/CT has high diagnostic accuracy in identifying recurrent UCa and positively impacts management of patients with suspected recurrent UCa [38, 39].

Imaging patterns of advanced urothelial cancer

Metastatic UCa most commonly involves lymph nodes, bones, and lungs followed by the liver (Figs. 3, 4). Less common sites of metastatic disease include pleura, soft tissue, adrenal glands, brain, and bowel (Fig. 3) [35, 36, 40–42]. On cross-sectional imaging, metastatic adenopathy presents with enlarged, bulky pelvic and retroperitoneal nodes, followed by intrathoracic, and less commonly, enlarged cervical nodes [35, 40]. A SUV > 2 and SUV > 4 have shown to have, respectively, high sensitivity (95%) and specificity (84.5%) for identifying metastatic adenopathy on FDG PET/CT [43].

Osseous metastases can be lytic, sclerotic or mixed, and rarely spinal cord compression due to epidural soft tissues or vertebral compression fracture [35, 40, 42]. Lung metastases present most commonly in the form of multiple lung nodules, and less commonly with lung consolidations or lymphangitic carcinomatosis, with nodular or irregular interlobular septal thickening [35, 40, 42]. Liver metastatic disease present with multiple hypodense on CT in the majority of cases [35, 40, 42]. In 10% of cases, hepatic metastatic disease can present as single hypoattenuating lesion [35]. Metastatic peritoneal disease takes the form of peritoneal nodules, thickening of the peritoneal folds, peritoneal stranding, serosal metastasis, and ascites. Bowel obstruction due to extensive serosal disease has been reported [35, 40, 42].

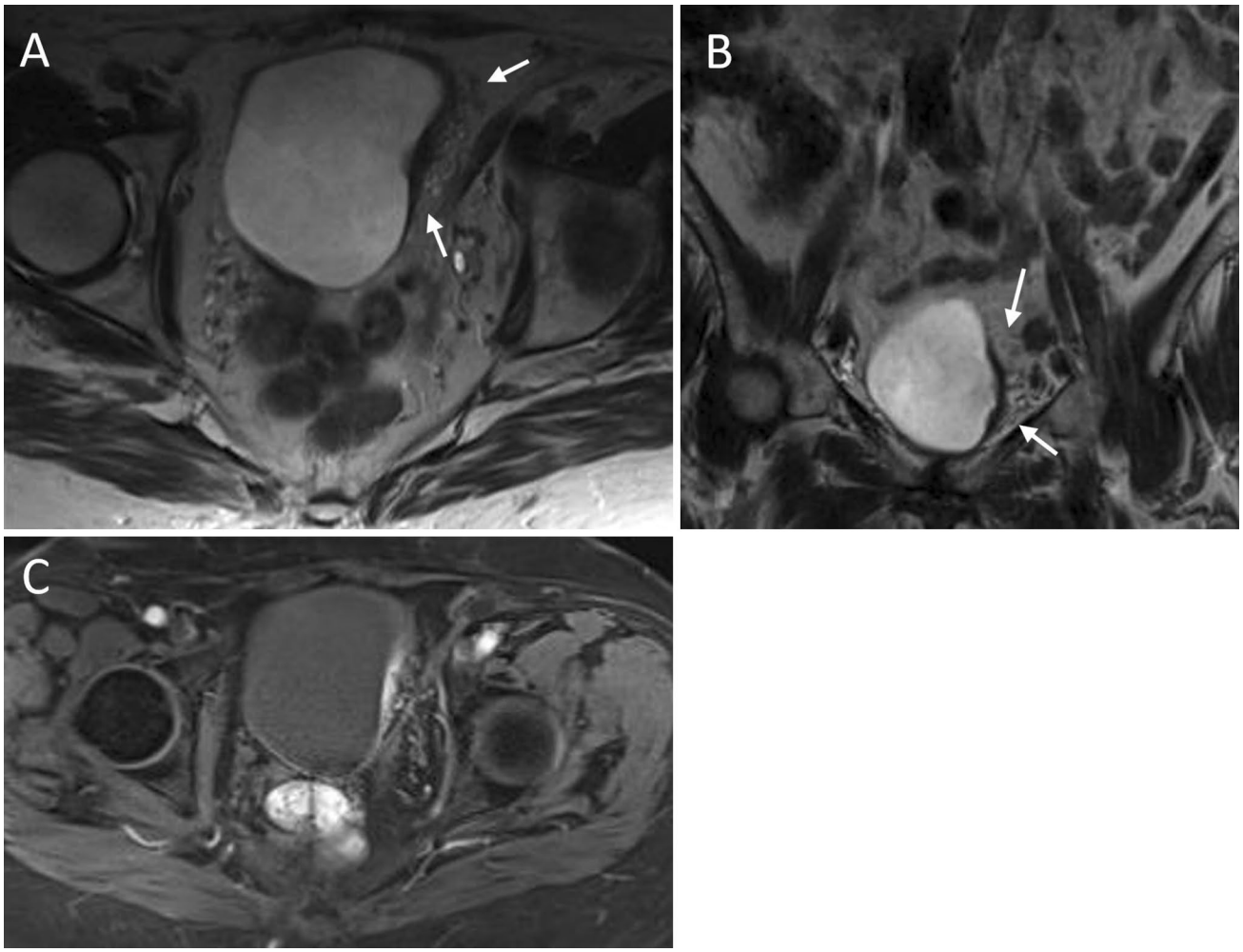

Fig. 2 89-year-old man with bladder cancer. Axial and coronal **a**, **b** T2-weighted image shows T2 hypointense thickening of the bladder wall and minimal stranding of the left paravescical fat (arrows). **c** Axial post-contrast T1-weighted image with fat saturation confirms left lateral muscle wall invasion of the bladder, representing locally advanced disease, possibly T3

In patients with bladder cancer and atypical histologic variants (e.g., tumors with squamous, glandular, micropapillary, plasmacytoid or sarcomatoid differentiation and poorly differentiated tumors), the disease may involve the peritoneum more commonly than in patients with 'pure' UCa (Fig. 4) [6, 40, 41]. In addition, patients with atypical histologic variants have a significantly shorter median metastasis-free interval in patients with 'pure' transitional cell carcinoma [6]. Regarding UTUCa, the pattern of metastatic spread is similar among the various histologic variants [42].

Systemic treatments for advanced urothelial cancer

Treatment selection in patients with advanced disease is based on cisplatin eligibility. Patients are treated with a cisplatin-based regimen unless there is renal insufficiency (creatinine clearance < 60 mL/min), poor Eastern Cooperative Oncology Group (ECOG) performance status (≥ 2), pre-existing peripheral neuropathy, hearing loss, or heart failure [44]. Table 2 summarizes the initial, termed first-line treatment regimens, and the subsequent treatment regimens for advanced UC.

Cisplatin-based combination chemotherapy remains the preferred first-line therapy for cisplatin-eligible patients and yields a median survival of 12 to 15 months. Approximately 50% of patients are cisplatin-ineligible and may be candidates for carboplatin-based chemotherapy, which is associated with suboptimal median survival of 8 to 9 months. Programmed death (PD)-ligand (L)-1 inhibitors—atezolizumab (Tecentriq, Genentech Oncology/Roche, San Francisco, CA), avelumab (Bavencio, EMD Serono, Inc. EMD Serono, Inc. and Pfizer Inc., Rockland, MA), and durvalumab (Imfinzi, Astrazeneca Pharmaceuticals LP, Wilmington, DE), —and PD-1 inhibitors—nivolumab (Opdivo, Bristol-Myers Squibb Company

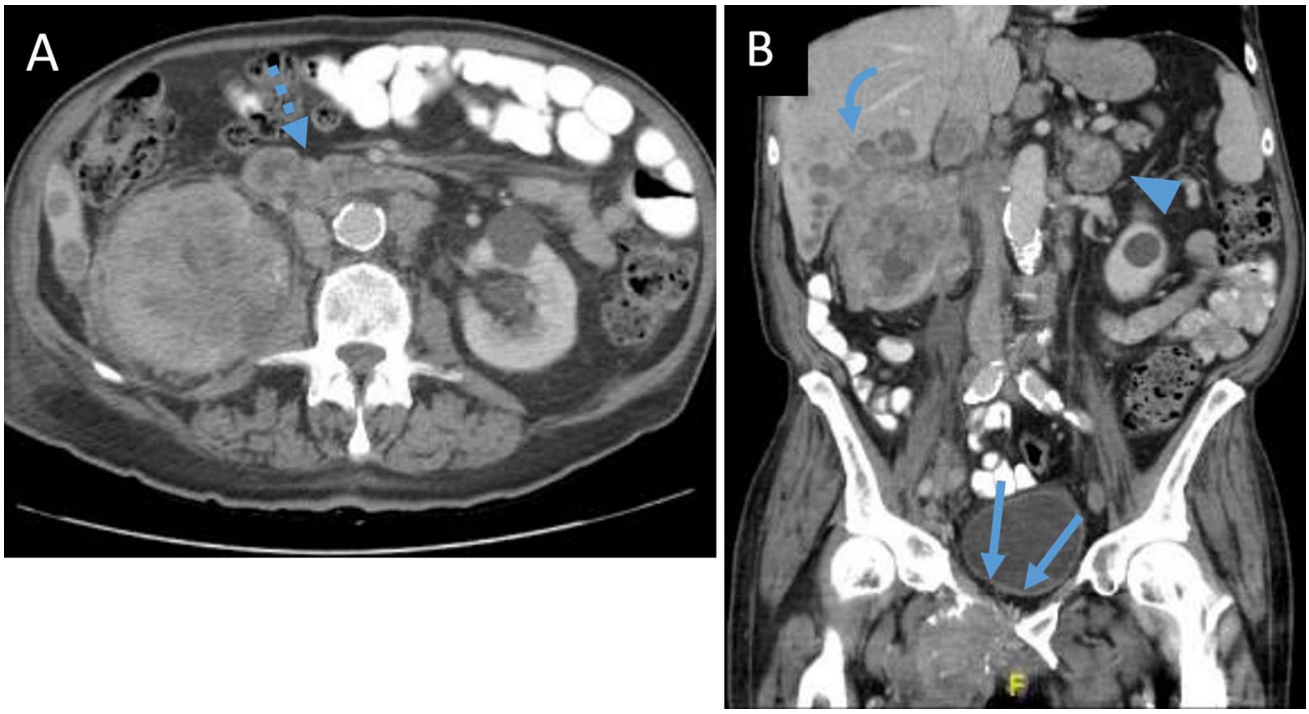

Fig. 3 77-year-old man with metastatic spread from urothelial carcinoma, arising from the right renal pelvis. **a** Axial post-contrast CT images show the primary renal pelvis mass with metastatic retroperitoneal lymph nodes (dashed arrow). **b** Coronal post-contrast CT image showing the primary right renal pelvis mass and the associated metastatic disease, with left adrenal lesion (arrowhead), liver lesions (curved arrow), and right pubic ramus lytic bone lesion (arrows)

Princeton, NJ) and pembrolizumab (Keytruda, Merck Sharp and Dohme Corp,/Merck, Whitehouse Station, NJ)—are approved for patients relapsing after platinum-based first-line therapy [45–50]. Atezolizumab and pembrolizumab are also approved as first-line therapy for cisplatin-ineligible advanced UCa with high tumor PD-L1 expression or platinum-ineligible patients regardless of PD-L1 expression [49, 51]. Despite durable responses in approximately 20% of post-platinum patients receiving PD1/PD-L1 inhibitor therapy, the median overall survival is 9 to 10 months [45–48, 50]. PD-1 and PD-L1 inhibitors are being combined with platinum-based combination chemotherapy and cytotoxic T-lymphocyte-associated (CTLA)-4 inhibiting immune modulators as first-line therapy in ongoing randomized phase III trials. Emerging agents in this space appear to provide incremental benefits including antibody drug conjugates (enfortumab vedotin, sacituzumab govitecan) and FGFR inhibitors (erdafitinib, rogaratinib) [52–54].

Drugs used to treat advanced urothelial cancer and their mechanism of action

Conventional chemotherapy

Various conventional chemotherapy agents are currently available for treatment of advanced UC, each with a different mechanism of action. These drugs can be classified as platinum-based antineoplastic agents (cisplatin and carboplatin), cytidine analogues (gemcitabine), antifolate agents (methotrexate and pemetrexed), vinca alkaloids (vinblastine), anthracyclines (doxorubicin), and nitrogen mustards (Ifosfamide) [5].

Platinum-based compounds bind to DNA and interfere with repair mechanisms causing DNA damage, subsequently inducing apoptosis [55, 56]. Folic acid analogs inhibit purine and pyrimidine DNA synthesis, ultimately inducing cell death [57, 58]. Vinca alkaloids, organic compounds derived from the

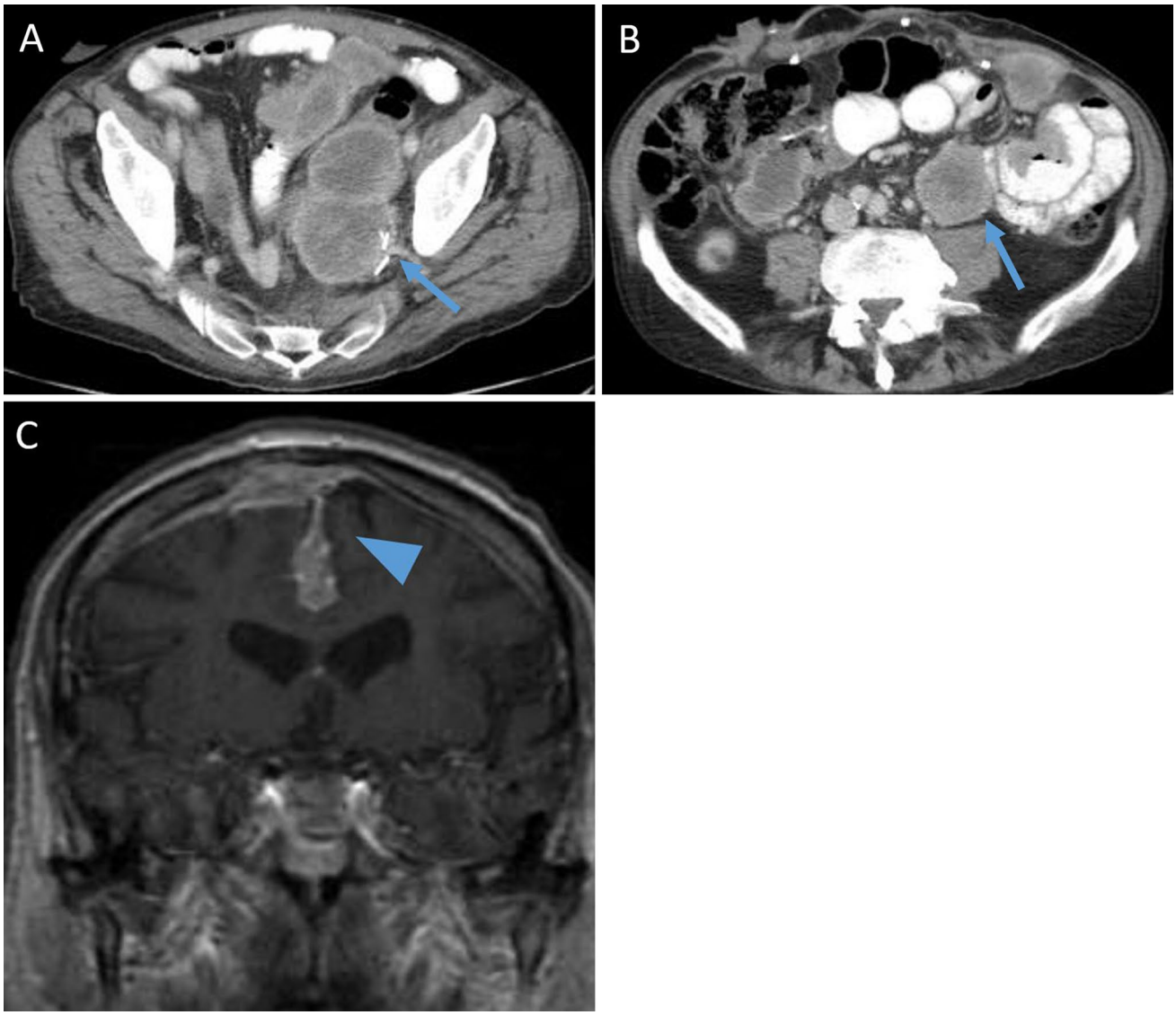

Fig. 4 67-year-old man with bladder urothelial carcinoma with sarcomatoid differentiation. **a**, **b** Axial post-contrast CT images showing multiple abdominal and pelvic metastatic deposits post-radical cystectomy. **c** Coronal T1-weighted post-contrast brain MRI demonstrate meningeal thickening and enhancement (arrowhead), representing meningeal metastatic disease

Madagascar periwinkle plant, bind to tubulin, a component of the microtubules forming the mitotic spindle apparatus, directly causing cell cycle arrest during metaphase and subsequent cell death [59]. Anthracyclines disrupt DNA repair mechanisms and damage cells through the generation of free radicals [60]. Nitrogen mustard metabolizes into a variety of active and potentially toxic metabolite which cause cell death through DNA alkylation and damage [61].

Programmed death-1/programmed death 1-ligand inhibitors

PD-1 and PD-L1 inhibitors encompass a group of immune checkpoint inhibitors whose activity is based on the inhibition of the PD-1, a receptor expressed on T cells, or its ligand, PD-L1, which is expressed on both tumor and immune cells. Together, PD-1 and PD-L1 suppress the activation of T cells, when these are activated by its circulating ligands in the context of infection or tumor [62, 63]. When PD-1 receptors are blocked, T cells initiate an inflammatory response against the tumor [64]. Thus far, three PD-L1 inhibitors—atezolizumab, durvalumab, and avelumab—and two PD-1 inhibitors—nivolumab and pembrolizumab—have received FDA approval for the treatment of advanced UC.

Table 2 First-line and subsequent systemic therapy for advanced urothelial carcinoma

	First-line regimens	Subsequent regimens
Cisplatin eligible	Gemcitabine and cisplatin DDMVAC with growth factor support	Pembrolizumab Atezolizumab Nivolumab Avelumab Durvalumab Paclitaxel or Docetaxel Gemcitabine Pemetrexed Alternate regimens *Paclitaxel* *Ifosfamide* *Methotrexate* *Ifosfamide, doxorubicine and gemcitabine* *Gemcitabine and paclitaxel* *Gemcitabine and cisplatin* *DDMVAC*
Cisplatin ineligible	Gemcitabine and carboplatin Atezolizumab[a] Pembrolizumab[b] Alternate regimens *Gemcitabine* *Gemcitabine and paclitaxel* *Ifosfamide, doxorubicine and Gemcitabine*	

DDMVAC dose dense methotrexate, vinblastine, doxorubicin, and cisplatin

[a]Treatment of locally advanced or metastatic UCa not eligible for cisplatin-containing therapy, and whose tumors express PD-L1 (PD-L1 stained tumor-infiltrating immune cells covering ≥ 5%)

[b]Treatment of locally advanced or metastatic urothelial carcinoma not eligible for cisplatin-containing therapy and whose tumors express PD-L1 (Combined Positive Score ≥ 10) or in or locally advanced or metastatic UCa not eligible for any platinum-containing chemotherapy regardless of PD-L1 status

Imaging assessment of advanced urothelial cancer treatment response

Conventional chemotherapy

Response assessment to conventional chemotherapy is based on size assessment of metastatic lesions (Table 3). Response to treatment is suggested where there is a decrease in lesion size; association of tumor shrinkage and survival has been demonstrated [65]. Currently, the Response Evaluation Criteria in Solid Tumors (RECIST 1,1) is the most widely used method to assess tumor response in solid malignancies treated with systemic therapies (Table 3) [66]. This method considers lesions measurable or non-measurable and uses unidimensional measurements to define response to treatment [66]. Although still widely used, RECIST 1.1 unidimensional tumor measurements vary between observers, and do not address the heterogeneity of response between metastatic lesions, which can occur when some lesions are responding to treatment while other are increasing in size [67]. To overcome this limitation, the use of tumor volume measurements to quantify entire tumor burden has been proposed as a marker for treatment benefit and prolonged survival [68].

Programmed death-1/programmed death 1-ligand inhibitors

Immune checkpoint inhibitors are associated with four specific patterns of treatment response: no new lesions and decrease in size of baseline lesion by 12 weeks; slow steady decline in tumor burden after initial stability of the metastatic lesions; initial increase in metastatic lesion size followed by decrease in tumor burden more than 12 weeks after the start of treatment; development of new metastatic lesions followed by decrease in tumor burden more than 12 weeks after the start of treatment [69]. Although an increase in lesion size ≥ 20%, termed "classical pseudoprogression" is rare in bladder cancer, other atypical responses, including an increase in less than 20% of the lesion size or the appearance of new lesions, are more common, occurring in 20% of patients with clinical benefit from immune checkpoint inhibitors (Fig. 5) [70]. Thus, awareness of the response pattern is crucial to avoid diagnosing disease progression when in fact the changes are due to pseudoprogression, in order to correctly identify patients which will have clinical benefit from immune checkpoint inhibitors. Specific immune-related response criteria that account for the different patterns of response compared to conventional chemotherapy have been developed to evaluate tumor response in patients treated with immune checkpoint inhibitors (Table 3) [68, 71, 72].

Imaging findings due to adverse events of treatment

Conventional chemotherapy

Conventional chemotherapy drugs are often the first agents used in advanced UCa and can be toxic; when used in

Table 3 Tumor response criteria for conventional chemotherapy agents and immune checkpoint inhibitors

RESPONSE	RECIST 1.1 [63]	irRECIST [66]	irRC [68]	iRECIST [69]
CR	Disappearance of all extranodal target and non-target lesions All pathological lymph nodes must be < 10 mm in short axis	Lymph nodes short axis should be < 10 mm No confirmation necessary	Disappearance of all lesions at two consecutive observations ≥ 4 weeks apart	Disappearance of all extranodal target and non-target lesions All pathological lymph nodes must be < 10 mm in short axis
PR	≥ 30% decrease in the SLD of target lesions compared to baseline No unequivocal progression of non-target disease No new lesions	≥ 30% decrease in the SLD of target lesions relative to baseline	↓ in in the SPD of target lesions ≥ 50% relative to baseline confirmed by a consecutive assessment at least 4 weeks after first documentation	≥ 30% decrease in the SLD of target lesions compared to baseline No unequivocal progression of non-target disease No new lesions
PD	≥ 20% increase in the SLD of target lesions AND absolute size increase of 5 mm in SLD compared with nadir OR Unequivocal increase of non-target lesions OR New lesions	≥ 20% increase in the SLD of target lesions relative to nadir and a minimum absolute increase of 5 mm	↑ in in the SPD of target lesions ≥ 25% relative to nadir (minimum recorded tumor burden)	≥ 20% + 5 mm absolute increase in tumor burden compared with nadir (minimum recorded tumor burden). Appearance of new lesions or progression of non-target lesions (iUPD) need to be confirmed 4–8 weeks later (iCPD). Clinical stability is considered when deciding whether to continue treatment after iUPD
SD	Does not meet above criteria	Does not meet above criteria	Does not meet above criteria	Does not meet above criteria

WHO World Health Organization, *RECIST* Response Evaluation Criteria in Solid Tumors, *irRECIST* immune-related RECIST, *irRC* immune-related response criteria, *iRECIST* immune RECIST, *CR* complete response, *PR* partial response, *SD* stable disease, *PD* progression of disease, *SLD* sum of the longest diameters, *SPD* sum of the products of diameters, *iUPD* immune unconfirmed progressive disease, *iCPD* immune confirmed progressive disease

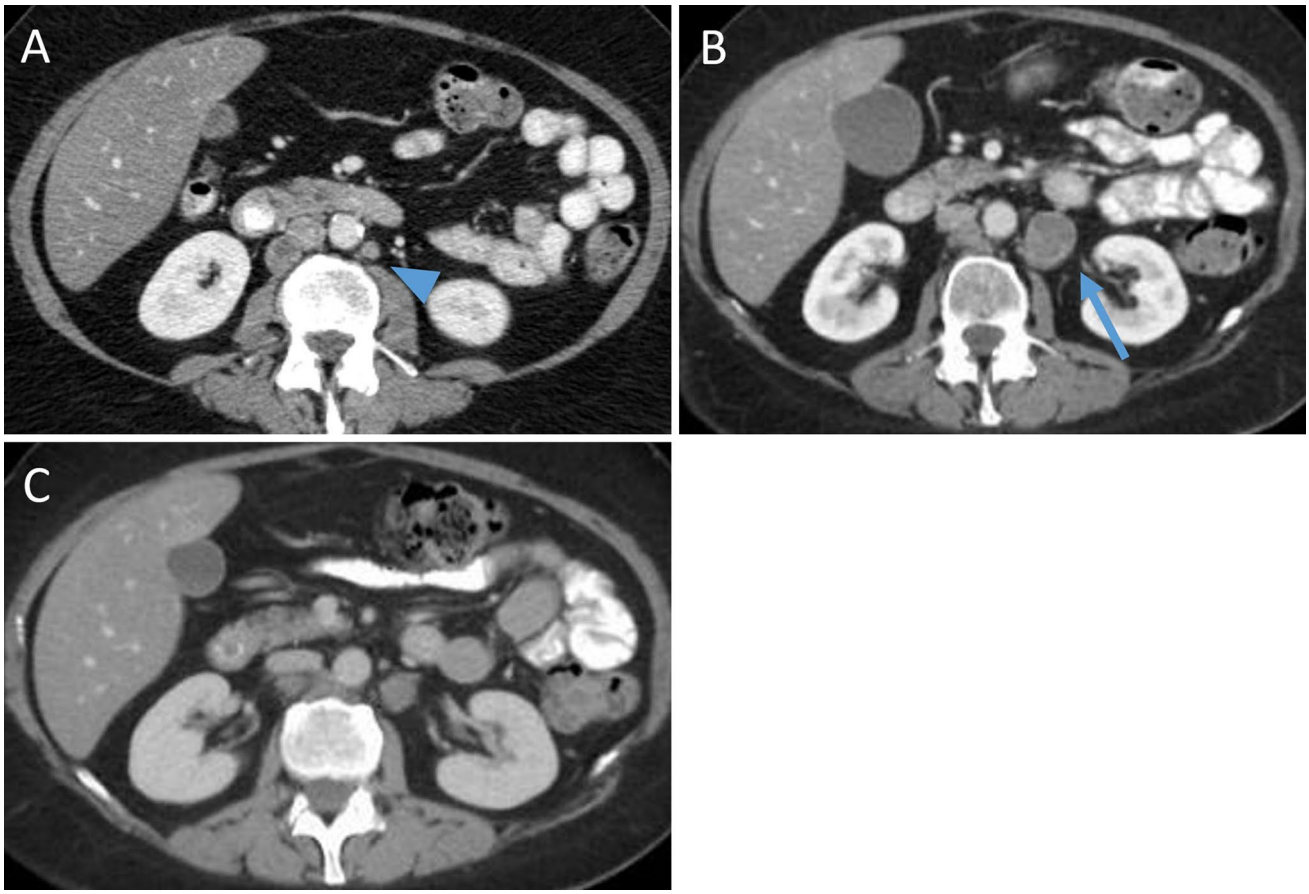

Fig. 5 57-year-old woman with metastatic bladder urothelial carcinoma treated with Nivolumab. (**a**) Axial post-contrast CT before starting Nivolumab shows a small left periaortic node which increased in size after Nivolumab was started (**b**) (arrow), suggesting the possibility of progression of disease. Patient was clinically stable and remained on Nivolumab. A follow-up CT performed after four weeks shows decreased size of the node (**b**), confirming pseudoprogression

combination, adverse events can arise from each agent used (Table 4) [73–86].

Cisplatin can cause acute kidney insufficiency in up to 30% of patients due to proximal tubular injury; renal ultrasound is used typically to exclude obstruction as the cause of the functional decline [73–76]. Gemcitabine, often used with cisplatin, can cause lung toxicity in up to 23% of patients; symptoms range from mild dyspnea to severe respiratory distress [73]. CT shows diffuse ground-glass changes with associated interlobular thickening, interstitial patchy consolidations, and diffuse alveolar opacities (Fig. 6) [73, 76]. Both cisplatin and gemcitabine are associated with the development of arterial thrombosis which can be manifest at CT as accelerated atherosclerosis [77].

Programmed death-1/programmed death 1-ligand inhibitors

Immune-related adverse events (irAEs) commonly observed on imaging include pulmonary, gastrointestinal, hepatobiliary, endocrine events, and sarcoid-like reactions (Table 4) [77–91]. Gastrointestinal irAEs present most commonly with diarrhea and can be observed in up to 20% of patients [88, 89]. A diffuse form results in colitis, enteritis, or enterocolitis [89]. A segmental form results in segmental colitis associated with diverticulosis [86]. Diffuse colitis and enteritis are characterized by fluid-filled bowel loops, mild bowel wall thickening, perivisceral mesenteric hyperemia, and mucosal hyperenhancement [88, 89]. Segmental colitis associated with diverticulosis is characterized by segmental wall thickening with associated pericolonic fat stranding that may be indistinguishable from diverticulitis [89].

IrAEs include hepatitis which typically presents with mildly enlarged, diffusely hypoattenuating, sometimes heterogeneously enhancing liver, periportal and gallbladder edema, and periportal lymphadenopathy. IrAEs also include pancreatitis, manifested as focal or diffuse pancreatic enlargement, decreased pancreatic parenchymal enhancement and peripancreatic stranding [89]. Pneumonitis can result from PD-1/PD-L1 inhibitors and

Table 4 Drug class, mechanism of actions, and selected toxicities following conventional chemotherapy agents used in advanced urothelial carcinoma

Drug	Drug class	Mechanism of action	Selected adverse events, clinical and imaging features [References]
Cisplatin Carboplatin[a]	Platinum	Platinum-based DNA damage	Hepatotoxicity [70, 75] Fat infiltration of the liver Cholestasis Acute pancreatitis [70, 76] Parenchymal enlargement Peripancreatic fluid collections Diffuse FDG-avidity of the pancreas on PET/CT Vascular toxicity [74] Occur in 9% of patients Arterial or venous thrombosis Nephrotoxicity [70] I nability to use iodinated contrast
Gemcitabine	Cytidine analogue	DNA polymerase inhibition	Pulmonary toxicity [70, 73] Occur in 23% of patients From mild to severe dyspnea and death Diffuse ground-glass opacities Interlobular thickening Interstitial patchy consolidations Diffuse alveolar opacities Capillary leak syndrome [70] Presentation with acute respiratory distress syndrome Diffuse ground-glass opacities Vascular toxicity [74] Arterial or venous thrombosis
Methotrexate Pemetrexed	Folic acid analog Antifolate analog	Folic acid metabolism inhibition Purine and pyrimidine synthesis blockade	Pulmonary toxicity - Methotrexate [70, 77]: Commonly < 1 year after starting treatment Bilateral interstitial and alveolar opacities Pleural effusions Pulmonary toxicity—pemetrexed [78, 79]: Interlobular thickening Diffuse ground-glass opacities Myelosuppression
Vinblastine	Vinca alkaloids	Binds to tubulin of microtubules Cell cycle arrest during metaphase	Large bowel ischemia [80, 81] Parietal pneumatosis Air in mesenteric and portal venous system Bowel wall thickening Mesenteric vascular engorgement and haziness Bowel loop dilation Pneumoperitoneum Neutropenia
Doxorubicin	Anthracyline drug	Disruption of DNA repair mechanisms Cell damage through free radicals' generation	Heart failure Occur in 15–60% of patients Dose dependent Screening with echocardiography or MUGA Myocardial edema, inflammation, fibrosis (cardiac MRI) [82]
Ifosfamide	Nitrogen mustard	DNA alkylation and damage	Acute hemorrhagic cystitis[b] [83] Focal or diffuse irregular bladder wall thickening Hyperdense layering material (CT) Edematous T2 hyperintensity of the wall (MRI) Neutropenia

Table 4 (continued)

Drug	Drug class	Mechanism of action	Selected adverse events, clinical and imaging features [References]
Pembrolizumab Nivolumab Atezolizumab Avelumab Durvalumab	Programmed Cell Death 1 inhibitors Programmed Cell Death ligand 1 inhibitors		Pneumonitis [84] Dryptogenic organizing pneumonia Peripheral basilar subpleural ground-glass changes Interlobular septal thickening mimicking NSIP Enterocolitis [85, 86] In up to 20% of patients Diffuse form Fluid-filled bowel loops Mild bowel wall thickening Perivisceral mesenteric hyperemia Mucosal hyperenhancement SCAD Segmental wall thickening with associated fat strand-ing Hepatitis [85, 86] Mild hepatomegaly Periportal and gallbladder edema Periportal lymphadenopathy Diffusely hypoattenuating liver parenchyma Heterogeneous parenchymal enhancement Pancreatitis [87] Parenchymal enlargement Peripancreatic fluid collections Diffuse FDG-avidity of the pancreas on PET/CT Thyroiditis [87] Increased size of the thyroid in acute phase May lead to hypotrophy of the thyroid and hypothy-roidism Adrenalitis [86, 87] Mild bilateral increase in size of adrenal glands Diffuse mild FDG-avidity of adrenal glands May lead to adrenal atrophy Sarcoid-like reaction [88] New or enlarging abdominal lymph nodes occurring early after starting treatment

NSIP non-specific interstitial pneumonia, *SCAD* segmental colitis associated with diverticulosis

[a]Carboplatin has milder nephrotoxic and gastrointestinal side effect [71, 72]

[b]To reduce incidence and severity is administered with mesna

can present with cryptogenic organizing pneumonia, with peripheral basilar subpleural ground-glass changes and interlobular septal thickening mimicking non-specific interstitial pneumonia (NSIP) (Fig. 7) [87]. Other less commonly observed irAEs include thyroiditis, adrenalitis, and hypophysitis [90]. In patients with new or enlarging thoracic or abdominal lymph nodes who recently started treatment with PD-1/PD-L1 inhibitors, the possibility of sarcoid-like reactions should be considered. In these patients, any change in treatment is best deferred until a follow-up study reveals that the nodes are smaller (indicating the drug reaction) or larger, indicating disease progression [91].

Future directions

Since there is currently no reliable predictor of treatment response, patients with advanced UCa may receive no benefit from a particular treatment regimen while incurring the often high costs of the drugs and suffering from their toxicities. A reliable biomarker of treatment response would help select which of the widely variable treatments are best, and allow different treatments to be selected in patients who are not responding [92].

Multiple molecular biomarkers are currently under investigation, including DNA mutation damage repair

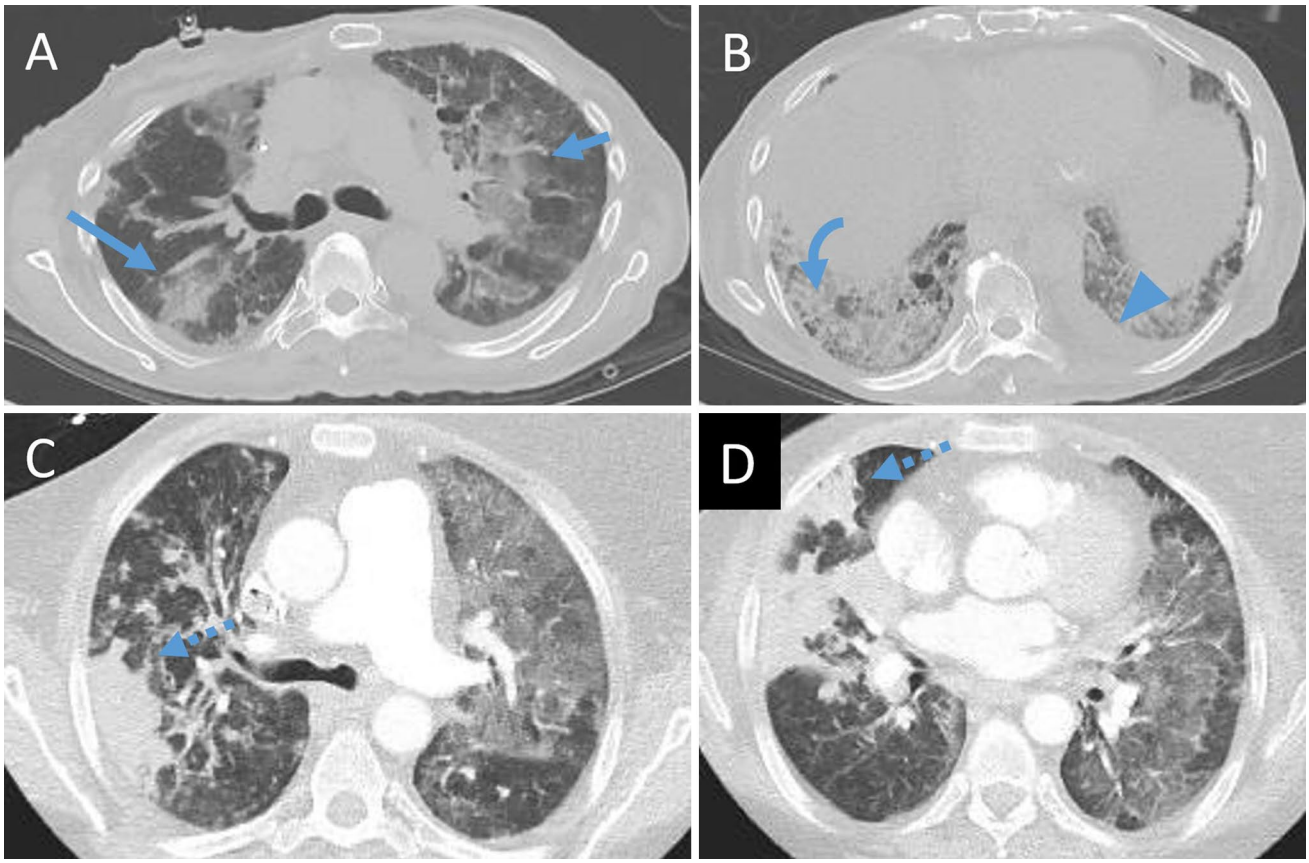

Fig. 6 Axial CT images of the chest in two different patients with Gemcitabine-associated pulmonary toxicity. **a**, **b** Axial CT of the chest shows bilateral patchy ground-glass opacities (arrows), interlobular thickening (curved arrow) and small left pleural effusions (arrowhead). **c**, **d** Axial CT of the chest on different patient shows diffuse bilateral ground-glass opacities and patchy consolidations (dashed arrows) in the right lung

pathways, receptor tyrosine kinases, gene expression markers, regulators of apoptosis, cellular mechanisms of drug uptake and transport, high tumor mutational burden, specific gene expression profiles (basal or luminal-infiltrated subtype and IFN-Y gene expression signature), and high levels of cytotoxic T lymphocytes infiltrating the tumor as well as PD-1/PD-L1 expression [92, 93].

Imaging-based biomarkers

In addition to genomic and cellular biomarkers, imaging-based non-invasive biomarkers show promise [94, 95]. Texture analysis is an imaging processing algorithm that allows quantification of underlying tumor heterogeneity by analyzing spatial distribution of heterogeneity in an image, typically at CT or MRI [96, 97]. Various reports have demonstrated the potential value of texture analysis as an imaging biomarker that may predict response to various treatment regimens in different cancer subtypes [98]. In advanced UCa, most studies focused on predicting response to systemic treatment [94, 95, 97]. In a study by Cha et al., multiple CT texture-based features helped predict the response of bladder cancer to systemic chemotherapy [94]. In another study of patients with advanced UCa treated with PD-1/PD-L1 inhibitors, CT texture analysis predicted progression within 1 year with high accuracy on first follow-up CT scan acquired at 2 months after initiating treatment [95].

Imaging-based radiomic models are currently under investigation, including models to predict nodal status in treatment naïve bladder cancer or to predict recurrence of bladder cancer after treatment [99, 100].

Conclusion

A number of novel therapies have become available for patients with advanced UCa, and improved understanding of mutational make-up of UCa would likely further impact treatment selection for these patients. Knowledge of the genomic landscape of UC, the patterns of spread of advanced UC, different systemic therapies available, and their patterns of treatment response and adverse events all

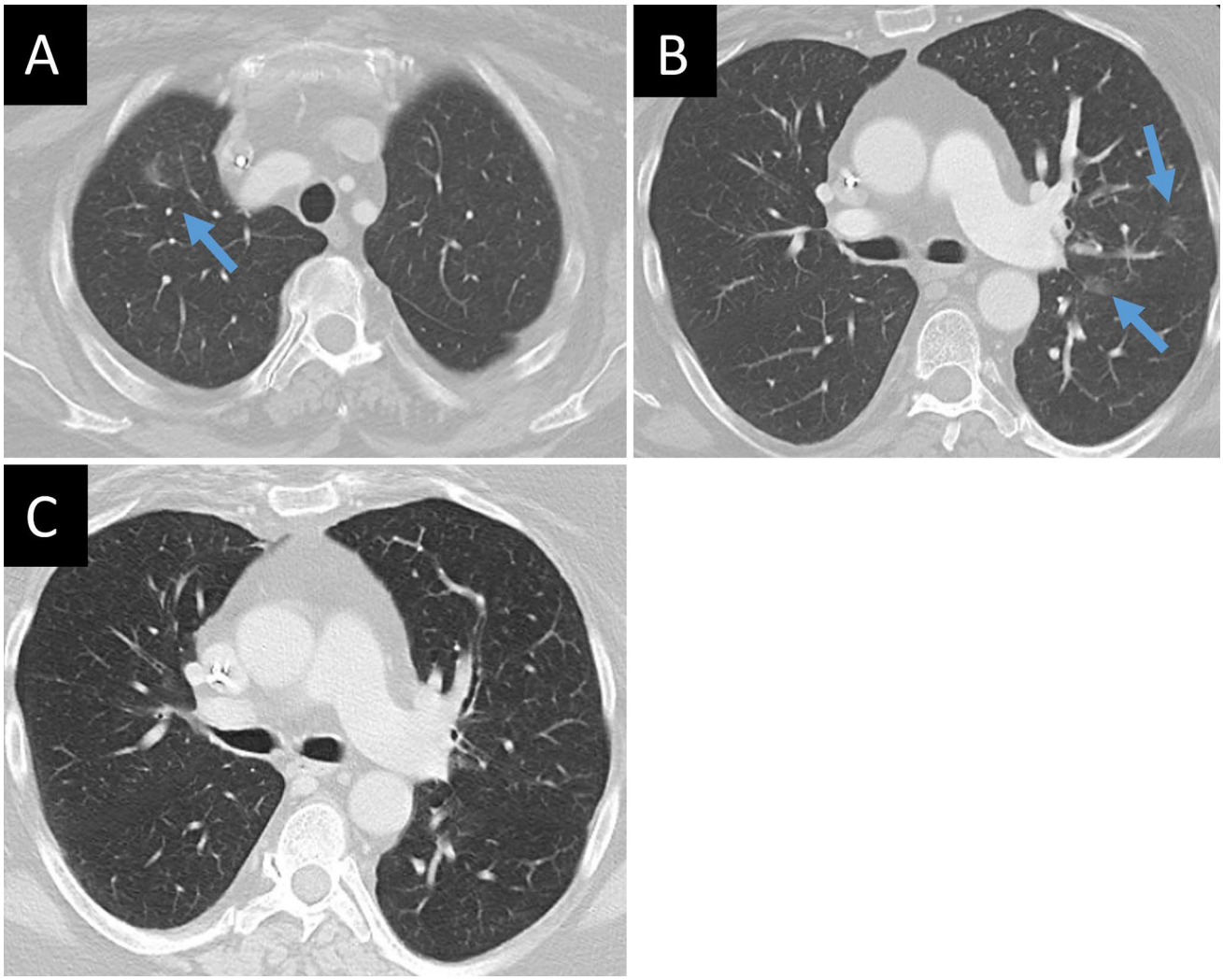

Fig. 7 56 year-old man with metastatic urothelial carcinoma treated with Atezolizumab. (**a**, **b**) Axial CT of the chest performed after starting treatment with the PD-L1 inhibitor show faint patchy ground-glass opacities (arrows), which resolved after Atezolizumab was discontinued (**c**) due to complete response after two years of treatment. Patient reported dyspnea on exertion and diagnosis of immune-related pneumonitis was given

help in understanding how imaging is best used to care for patients with advanced UC.

Compliance with ethical standards

Conflict of interest Guru P. Sonpavde, MD: Consultant for BMS, Exelixis, Bayer, Sanofi, Pfizer, Novartis, Eisai, Janssen, Amgen, Astrazeneca, Merck, Genentech, EMD Serono, Astellas/Agensys; Research support to institution from Astrazeneca, Bayer, Amgen, Boehringer-Ingelheim, Janssen, Merck, Sanofi, Pfizer; Author for Uptodate; Steering committee for Astrazeneca, BMS, Bavarian Nordic; Speaker for Onclive; Research to Practice; Physician Education Resource (PER). Atul B. Shinagare, MD: Relevant: none; unrelated: Consultant, Arog Pharmaceuticals, Virtualscopics. All other authors have no conflict of interest.

Ethical approval This article does not contain any studies with human participants or animals performed by any of the authors.

Informed consent Statement of informed consent is not applicable since the manuscript does not contain any patient data.

References

1. Rouprêt M, Babjuk M, Compérat E, et al (2015) European Association of Urology guidelines on upper urinary tract urothelial cell carcinoma: 2015 update. Eur Urol 68:868–879
2. Leow JJ, Chong KT, Chang SL, et al (2016) Upper tract urothelial carcinoma: a different disease entity in terms of management ESMO Open. https://doi.org/10.1136/esmoopen-2016-000126

3. Siegel RL, Miller KD, Jemal A (2019) Cancer statistics, 2019. CA Cancer J Clin 69(1):7-34
4. Lalani AA, Sonpavde GP (2019) Systemic treatments for metastatic urothelial carcinoma. Expert Opin Pharmacother 20(2):201-208
5. Robertson AG, Kim J, Al-Ahmadie H, et al (2017) Comprehensive molecular characterization of muscle-invasive bladder cancer. Cell 171: 540-556
6. Shinagare AB, Ramaiya NH, Jagannathan JP, Fennessy FM, Taplin ME, Van den Abbeele AD (2011) Metastatic pattern of bladder cancer: correlation with the characteristics of the primary tumor. AJR Am J Roentgenol 196(1):117-122
7. Spiess PE, Agarwal N, Bangs R, et al (2017) Bladder Cancer, Version 5.2017, NCCN Clinical Practice Guidelines in Oncology. J Natl Compr Canc Netw 15(10):1240-1267
8. Choe J, Braschi-Amirfarzan M, Tirumani SH, et al (2017) Updates for the radiologist in non-muscle-invasive, muscle-invasive, and metastatic bladder cancer. Abdom Radiol (NY) 42(11):2710-2724
9. Moss TJ, Qi Y, Xi L, et al (2017) Comprehensive Genomic Characterization of Upper Tract Urothelial Carcinoma. Eur Urol 72(4):641-649
10. Humphrey PA, Moch H, Cubilla AL, Ulbright TM, Reuter VE (2016) The 2016 WHO Classification of Tumours of the Urinary System and Male Genital Organs-Part B: Prostate and Bladder Tumours. Eur Urol 70(1):106-119
11. Sanli O, Dobruch J, Knowles MA, et al (2017) Bladder cancer. Nat Rev Dis Primers 3:17022
12. Audenet F, Attalla K, Sfakianos JP (2018) The evolution of bladder cancer genomics: What have we learned and how can we use it? Urol Oncol 36(7):313-320
13. Vogelstein B, Papadopoulos N, Velculescu VE, Zhou S, Diaz LA, Kinzler KW (2013) Cancer genome landscapes. Science 339(6127):1546–1558
14. Pietzak EJ, Bagrodia A, Cha EK, et al (2017) Next-generation sequencing of nonmuscle invasive bladder cancer reveals potential biomarkers and rational therapeutic targets. Eur Urol DOI:https://doi.org/10.1016/j.eururo.2017.05.032
15. Lawrence MS, Stojanov P, Polak P, et al (2013) Mutational heterogeneity in cancer and the search for new cancer-associated genes. Nature 499:214-218
16. Damrauer JS, Hoadley KA, Chism DD, et al (2014) Intrinsic subtypes of high- grade bladder cancer reflect the hallmarks of breast cancer biology. Proc Natl Acad Sci USA 111:3110–3115
17. Rebouissou S, Bernard-Pierrot I, deReyniès A,et al (2014) EGFR as a potential therapeutic target for a subset of muscle-invasive bladder cancers presenting a basal-like phenotype Sci Transl Med 244ra91–1
18. Choi W, Porten S, Kim S, et al (2014) Identification of distinct basal and luminal subtypes of muscle-invasive bladder cancer with different sensitivities to frontline chemotherapy. Cancer Cell 25:152–65
19. Eriksson P, Sjödahl G, Chebil G, Liedberg F, Höglund M (2017) HER2 and EGFR amplification and expression in urothelial carcinoma occurs in distinct biological and molecular contexts. Oncotarget 8(30):48905-48914
20. Seiler R, Ashab HA, Erho N, et al (2017) Impact of Molecular Subtypes in Muscle-invasive Bladder Cancer on Predicting Response and Survival after Neoadjuvant Chemotherapy. Eur Urol 72(4):544-554
21. Rosenberg JE, Hoffman-Censits J, Powles T, et al (2016) Atezolizumab in patients with locally advanced and metastatic urothelial carcinoma who have progressed following treatment with platinum based chemotherapy: A single-arm, multicentre, phase 2 trial. Lancet 387:1909–1920
22. Mak MP, Tong P, Diao L, et al (2015) A Patient-Derived, Pan-Cancer EMT Signature Identifies Global Molecular Alterations and Immune Target Enrichment Following Epithelial-to-Mesenchymal Transition. Clin Cancer Res 22(3):609-620
23. Karkera JD, Martinez Cardona G, Bell K, et al (2017) Oncogenic characterization and pharmacologic sensitivity of activating fibroblast growth factor receptor (FGFR) genetic alterations to the selective FGFR inhibitor erdafitinib. Mol Cancer Ther 16:1717–1726
24. Kiss B, Wyatt AW, Douglas J, et al (2017) Her2 alterations in muscle-invasive bladder cancer: Patient selection beyond protein expression for targeted therapy. Sci Rep7:42713
25. Groenendijk FH, de Jong J, Fransen van de Putte EE, et al (2016) ERBB2 Mutations Characterize a Subgroup of Muscle-invasive Bladder Cancers with Excellent Response to Neoadjuvant Chemotherapy. Eur Urol 69(3):384-488
26. Tan TZ, Rouanne M, Tan KT, Huang RY, Thiery JP (2018) Molecular Subtypes of Urothelial Bladder Cancer: Results from a Meta-cohort Analysis of 2411 Tumors. Eur Urol 75(3):423-432
27. Kim J, Kwiatkowski D, McConkey DJ, et al (2019) The Cancer Genome Atlas Expression Subtypes Stratify Response to Checkpoint Inhibition in Advanced Urothelial Cancer and Identify a Subset of Patients with High Survival Probability. Eur Urol https://doi.org/10.1016/j.eururo.2019.02.017
28. Wang L, Saci A, Szabo PM, et al (2018) EMT- and stroma-related gene expression and resistance to PD-1 blockade in urothelial cancer. Nat Commun 9:3503
29. Mariathasan S, Turley SJ, Nickles D, et al (2018) TGFbeta attenuates tumour response to PD-L1 blockade by contributing to exclusion of T cells. Nature 554:544-548
30. Nassar AH, Umeton R, Kim J, et al (2018) Mutational analysis of 472 urothelial carcinoma across grades and anatomic sites. Clin Cancer Res https://doi.org/10.1158/1078-0432.ccr-18-3147
31. National Comprehensive Cancer Network. NCCN Clinical Practice Guidelines in Oncology (NCCN Guidelines) Version 1.2019 – December 20, 2018. https://www.nccn.org/professionals/physician_gls/pdf/bladder.pdf. Accessed February 1, 2019.
32. Royal College of Radiologists (2014) Bladder cancer and other urothelial tumours, in: Recommendations for cross-sectional imaging in cancer management. 2nd edn, pp 3-8
33. Ghafoori M, Shakiba M, Ghiasi A, Asvadi N, Hosseini K, Alavi M (2013) Value of MRI in local staging of bladder cancer. Urol J 10:866–872
34. Lee CH, Tan CH, Faria SC, Kundra V (2017) Role of Imaging in the Local Staging of Urothelial Carcinoma of the Bladder. AJR Am J Roentgenol 208(6):1193-1205
35. Shinagare AB, Sadow CA, Silverman SG (2013) Surveillance of patients with bladder cancer following cystectomy: yield of CT urography. Abdom Imaging 38(6):1415-1421
36. Anderson TS, Regine WF, Kryscio R, Patchell RA (2003) Neurologic complications of bladder carcinoma: a review of 359 cases. Cancer;97(9):2267-2272
37. Alfred Witjes J, Lebret T, Compérat EM, et al (2017) Updated 2016 EAU Guidelines on Muscle-invasive and Metastatic Bladder Cancer. Eur Urol 71(3):462-475
38. Zattoni F, Incerti E, Colicchia M, et al (2018) Comparison between the diagnostic accuracies of 18F-fluorodeoxyglucose positron emission tomography/computed tomography and conventional imaging in recurrent urothelial carcinomas: a retrospective, multicenter study. Abdom Radiol (NY) 43(9):2391-2399
39. Zattoni F, Incerti E, Dal Moro F, et al (2019) 18F-FDG PET/CT and Urothelial Carcinoma: Impact on Management and Prognosis-A Multicenter Retrospective Study. Cancers (Basel) 11(5):700
40. Wallmeroth A, Wagner U, Moch H, Gasser TC, Sauter G, Mihatsch MJ (1999) Patterns of metastasis in muscle-invasive

bladder cancer (pT2–4): an autopsy study on 367 patients. Urol Int 62:69–75
41. Sengeløv L, Kamby C, von der Maase H (1996) Pattern of metastases in relation to characteristics of primary tumor and treatment in patients with disseminated urothelial carcinoma. J Urol 155:111–114
42. Shinagare AB, Fennessy FM, Ramaiya NH, Jagannathan JP, Taplin ME, Van den Abbeele AD (2011) Urothelial cancers of the upper urinary tract: metastatic pattern and its correlation with tumor histopathology and location. J Comput Assist Tomogr 35(2):217-222
43. Vind-Kezunovic S, Bouchelouche K, Ipsen P, Høyer S, Bell C, Bjerggaard Jensen J (2019) Detection of Lymph Node Metastasis in Patients with Bladder Cancer using Maximum Standardised Uptake Value and 18F-fluorodeoxyglucose Positron Emission Tomography/Computed Tomography: Results from a High-volume Centre Including Long-term Follow-up. Eur Urol Focus 5(1):90-96
44. Galsky MD, Hahn NM, Rosenberg J, et al (2011) A consensus definition of patients with metastatic urothelial carcinoma who are unfit for cisplatin-based chemotherapy. Lancet Oncol 12:211-214
45. Sharma P, Callahan MK, Bono P, et al (2016) Nivolumab monotherapy in recurrent metastatic urothelial carcinoma (CheckMate 032): a multicentre, open-label, two-stage, multi-arm, phase 1/2 trial. Lancet Oncol 17(11):1590-1598
46. Massard C, Gordon MS, Sharma S, et al (2016) Safety and Efficacy of Durvalumab (MEDI4736), an Anti-Programmed Cell Death Ligand-1 Immune Checkpoint Inhibitor, in Patients With Advanced Urothelial Bladder Cancer. J Clin Oncol 34:3119-3125
47. Bellmunt J, de Wit R, Vaughn DJ, et al (2017) Pembrolizumab as Second-Line Therapy for Advanced Urothelial Carcinoma. N Engl J Med 376:1015-1026
48. Patel MR, Ellerton J, Infante JR, et al (2018) Avelumab in metastatic urothelial carcinoma after platinum failure (JAVELIN Solid Tumor): pooled results from two expansion cohorts of an open-label, phase 1 trial. Lancet Oncol 19:51-64
49. Balar AV, Galsky MD, Rosenberg JE, et al (2017) Atezolizumab as first-line treatment in cisplatin-ineligible patients with locally advanced and metastatic urothelial carcinoma: a single-arm, multicentre, phase 2 trial. Lancet 389:67-76
50. Powles T, Duran I, van der Heijden MS, et al (2018) Atezolizumab versus chemotherapy in patients with platinum-treated locally advanced or metastatic urothelial carcinoma (IMvigor211): a multicentre, open-label, phase 3 randomised controlled trial. Lancet 391:748-757
51. Balar AV, Castellano D, O'Donnell PH, et al (2017) First-line pembrolizumab in cisplatin-ineligible patients with locally advanced and unresectable or metastatic urothelial cancer (KEYNOTE-052): a multicentre, single-arm, phase 2 study. Lancet Oncol 18(11):1483-1492
52. Petrylak DP PR, Zhang J, et al (2017) A Phase I Study of Enfortumab Vedotin: Updated Analysis of Patients with Metastatic Urothelial Cancer. J Clin Oncol 35 (suppl; abstr 106)
53. Tagawa ST, Faltas BM, Lam ET, et al (2019) Sacituzumab govitecan (IMMU-132) in patients with previously treated metastatic urothelial cancer (mUC): Results from a phase I/II study. J Clin Oncol 37:354-354
54. Siefker-Radtke AO, Necchi A, Park SH, et al (2018) First results from the primary analysis population of the phase 2 study of erdafitinib (ERDA; JNJ-42756493) in patients (pts) with metastatic or unresectable urothelial carcinoma (mUC) and FGFR alterations (FGFRalt). J Clin Oncol 36:4503-4503
55. Dasari S, Tchounwou PB (2014) Cisplatin in cancer therapy: molecular mechanisms of action. Eur J Pharmacol 740:364–378
56. Rosenberg B, Camp LV, Krigas T (1965) Inhibition of cell division in escherichia coli by electrolysis products from a platinum electrode. Nature 205(4972):698–699
57. Tian H, Cronstein BN (2007) Understanding the mechanisms of action of methotrexate: implications for the treatment of rheumatoid arthritis. Bull NYU Hosp Jt Dis 65(3):168-173
58. Hagner N, Joerger M (2010) Cancer chemotherapy: targeting folic acid synthesis. Cancer Manag Res 2:293-301
59. Moudi M, Go R, Yien CY, Nazre M (2013) Vinca alkaloids. Int J Prev Med 4(11):1231–1235
60. Thorn CF, Oshiro C, Marsh S, et al (2011) Doxorubicin pathways: pharmacodynamics and adverse effects. Pharmacogenet Genomics 21(7):440-446
61. Tascilar M, Loos WJ, Seynaeve C, Verweij J, Sleijfer S. The pharmacologic basis of ifosfamide use in adult patients with advanced soft tissue sarcomas. Oncologist. 2007;12(11):1351-1360
62. Fife BT, Pauken KE, Eagar TN, et al. Interactions between programmed death-1 and programmed death ligand-1 promote tolerance by blocking the T cell receptor-induced stop signal. Nat immunol 2009;10(11):1185-1192
63. Dong H, Strome SE, Salomao DR, et al. Tumor-associated B7-H1 promotes T-cell apoptosis: a potential mechanism of immune evasion. Nat Med 2002;8(8):793-800
64. Dermani FK, Samadi P, Rahmani G, Kohlan AK, Najafi R. PD-1/PD-L1 immune checkpoint: Potential target for cancer therapy. J Cell Physiol 2019 234(2):1313-1325.
65. Tang PA, Bentzen SM, Chen EX, Siu LL (2007) Surrogate end points for median overall survival in metastatic colorectal cancer: literature-based analysis from 39 randomized controlled trials of first-line chemotherapy. J Clin Oncol 25(29):4562-4568
66. Eisenhauer EA, Therasse P, Bogaerts J, et al (2009) New response evaluation criteria in solid tumours: revised RECIST guideline (version 1.1). Eur J Cancer 45:228-247.
67. Nishino M (2018) Tumor Response Assessment for Precision Cancer Therapy: Response Evaluation Criteria in Solid Tumors and Beyond. American Society of Clinical Oncology Educational Book 38:1019-1029
68. Nishino M, Hatabu H, Johnson BE, McLoud TC (2014) State of the art: Response assessment in lung cancer in the era of genomic medicine. Radiology 271(1):6-27
69. Wolchok JD, Hoos A, O'Day S, et al (2009) Guidelines for the evaluation of immune therapy activity in solid tumors: immune-related response criteria. Clin Cancer Res 15(23):7412-7420
70. Thomas R, Somarouthu B, Alessandrino F, Kurra V, Shinagare AB (2019) Atypical Response Patterns in Patients Treated With Nivolumab. AJR Am J Roentgenol 1-5
71. Nishino M, Giobbie-Hurder A, Gargano M, Suda M, Ramaiya NH, Hodi FS (2013) Developing a common language for tumor response to immunotherapy: immune-related response criteria using unidimensional measurements. Clin Cancer Res 19(14):3936–3943
72. Seymour L, Bogaerts J, Perrone A, et al (2017) iRECIST: guidelines for response criteria for use in trials testing immunotherapeutics. Lancet Oncol 18(3):e143–e152
73. Torrisi JM, Schwartz LH, Gollub MJ, et al. (2011) CT findings of chemotherapy-induced toxicity: what radiologists need to know about the clinical and radiologic manifestations of chemotherapy toxicity. Radiology 258(1):41–56
74. Lokich J, Anderson N (1998) Carboplatin versus cisplatin in solid tumors: an analysis of the literature. Ann Oncol 9(1):13-21
75. De Santis M, Bellmunt J, Mead G, et al (2011) Randomized phase II/III trial assessing gemcitabine/carboplatin and methotrexate/carboplatin/vinblastine in patients with advanced urothelial cancer who are unfit for cisplatin-based chemotherapy: EORTC study 30986. J Clin Oncol 30(2):191-199

76. Chi D-C, Brogan F, Turenne I, et al. (2012) Gemcitabine-induced pulmonary toxicity. Anticancer Res 32(9):4147–4149
77. Rohatgi S, Jagannathan JP, Rosenthal MH, et al. (2014) Vascular toxicity associated with chemotherapy and molecular targeted therapy: what should a radiologist know? AJR 203(6):1353–1362
78. King PD, Perry MC (2001) Hepatotoxicity of chemotherapy. Oncologist 6(2):162–176
79. Trivedi CD, Pitchumoni CS (2005) Drug-induced pancreatitis: an update. J Clin Gastroenterol 39(8):709–716
80. Arakawa H, Yamasaki M, Kurihara Y, Yamada H, Nakajima Y (2003) Methotrexate-induced pulmonary injury: serial CT findings. J Thorac Imaging 18(4):231-236
81. Adjei AA (2000). Pemetrexed: a multitargeted antifolate agent with promising activity in solid tumors. Ann Oncol 11(10):1335-1341
82. Kim KH, Song SY, Lim KH, et al (2013) Interstitial Pneumonitis after Treatment with Pemetrexed for Non-small Cell Lung Cancer. Cancer Res Treat 45(1):74-77
83. Rha SE, Ha HK, Lee SH, et al (2000) CT and MR imaging findings of bowel ischemia from various primary causes. Radiographics 20(1):29-42
84. Longstreth GF, Yao JF (2010) Diseases and drugs that increase risk of acute large bowel ischemia. Clin Gastroenterol Hepatol 8(1):49-54
85. Hendel RC, Patel MR, Kramer CM, et al (2006) ACCF/ACR/SCCT/SCMR/ASNC/NASCI/SCAI/SIR 2006 appropriateness criteria for cardiac computed tomography and cardiac magnetic resonance imaging: a report of the American College of Cardiology Foundation Quality Strategic Directions Committee Appropriateness Criteria Working Group, American College of Radiology, Society of Cardiovascular Computed Tomography, Society for Cardiovascular Magnetic Resonance, American Society of Nuclear Cardiology, North American Society for Cardiac Imaging, Society for Cardiovascular Angiography and Interventions, and Society of Interventional Radiology. J Am Coll Cardiol 48(7):1475-1497
86. Wong-you-cheong JJ, Woodward PJ, Manning MA et al (2006) From the archives of the AFIP: Inflammatory and nonneoplastic bladder masses: radiologic-pathologic correlation. Radiographics. 26 (6): 1847-1868
87. Nishino M, Ramaiya NH, Awad MM, et al (2016) PD-1 Inhibitor-Related Pneumonitis in Advanced Cancer Patients: Radiographic Patterns and Clinical Course. Clin Cancer Res 22(24):6051-6060
88. Mekki A, Dercle L, Lichtenstein P, et al (2018) Detection of immune-related adverse events by medical imaging in patients treated with anti-programmed cell death 1. Eur J Cancer 96:91-104
89. Alessandrino F, Sahu S, Nishino M, et al (2019) Frequency and imaging features of abdominal immune-related adverse events in metastatic lung cancer patients treated with PD-1 inhibitor. Abdom Radiol (NY). https://doi.org/10.1007/s00261-019-01935-2
90. Alessandrino F, Shah HJ, Ramaiya NH (2018) Multimodality imaging of endocrine immune related adverse events: a primer for radiologists. Clin Imaging 50:96-103
91. Cheshire SC, Board RE, Lewis AR, Gudur LD, Dobson MJ (2018) Pembrolizumab-induced Sarcoid-like Reactions during Treatment of Metastatic Melanoma. Radiology 14:180572
92. Wezel F, Vallo S, Roghmann F, Young Academic Urologist Urothelial Carcinoma Group of the European Association of Urology (2017) Do we have biomarkers to predict response to neoadjuvant and adjuvant chemotherapy and immunotherapy in bladder cancer?. Transl Androl Urol 6(6):1067-1080
93. Zhu J, Armstrong AJ, Friedlander TW, et al (2018) Biomarkers of immunotherapy in urothelial and renal cell carcinoma: PD-L1, tumor mutational burden, and beyond. J Immunother Cancer 6(1):4
94. Cha KH, Hadjiiski L, Chan H-P, et al. (2017) Bladder Cancer Treatment Response Assessment in CT using Radiomics with Deep-Learning. Sci Rep 7:8738
95. Alessandrino F, Gujrathi R, Nassar AH, et al (2019) Predictive Role of Computed Tomography Texture Analysis in Patients with Metastatic Urothelial Cancer Treated with Programmed Death-1 and Programmed Death-ligand 1 Inhibitors. Eur Urol Oncol https://doi.org/10.1016/j.euo.2019.02.002
96. Ganeshan B, Miles KA (2013) Quantifying tumour heterogeneity with CT. Cancer Imaging 13:140-149
97. Thomas R, Qin L, Alessandrino F, et al (2018) A review of the principles of texture analysis and its role in imaging of genitourinary neoplasms. Abdom Radiol (NY) https://doi.org/10.1007/s00261-018-1832-5
98. Lubner MG, Smith AD, Sandrasegaran K, Sahani DV, Pickhardt P (2017) CT Texture Analysis: Definitions, Applications, Biologic Correlates, and Challenges. RadioGraphics 37:5:1483-503
99. Xu X, Wang H, Du P, et al (2019) A predictive nomogram for individualized recurrence stratification of bladder cancer using multiparametric MRI and clinical risk factors. J Magn Reson Imaging https://doi.org/10.1002/jmri.26749
100. Wu S, Zheng J, Li Y, et al (2017) A Radiomics Nomogram for the Preoperative Prediction of Lymph Node Metastasis in Bladder Cancer. Clin Cancer Res 23(22):6904-6911